Harnessing Peptides against lead pollution and poisoning: Achievements and prospects

Sauser, Luca ; Shoshan, Michal S

DOI: https://doi.org/10.1016/j.jinorgbio.2020.111251

Harnessing Peptides Against Lead Pollution and Poisoning: Achievements and Prospects

Luca Sauser and Michal S. Shoshan*

Department of Chemistry, University of Zurich, Winterthurerstrasse 190, 8057 Zurich, Switzerland

michal.shoshan@chem.uzh.ch

Abstract

Among the broad applicability of peptides in numerous aspects of life and technologies, their interactions with lead (Pb), one of the most harmful substances to the environment and health, are constantly explored. So far, peptides were developed for environmental remediation of Pb-contaminations by various strategies such as hydrogelation and surface display. They were also designed for Pb detection and sensing by electrochemical and fluorescent methods and for modeling natural proteins that involve in mechanisms by which Pb is toxic. This review aims at summarizing selected examples of these applications, manifesting the enormous potential of peptides in the combat against Pb pollution. Nevertheless, the absence of new medicinal treatments against Pb poisoning that are based on peptides is noticeable. An overview of previous achievements utilizing Pb-peptide interactions towards various goals is presented and can be therefore leveraged to construct a useful toolbox for the design of smart peptides as next-generation therapeutics against Pb.

Keywords

Lead, Pb-poisoning, peptides, chelation therapy, remediation, detection

Highlights

- Peptide-based systems can remediate Pb in various techniques.
- Peptides are harnessed for Pb detection in complex environments such as cells and blood.
- Although being highly important, no new Pb chelating agents are reported.
- Smart design of peptides can be utilized for next-generation treatments of Pb poisoning.

1 Introduction

Lead (Pb) is one of the most abundant and toxic metals in the environment. Pb is released in significant quantities into the air, soil and water through industrial use and from household items, such as Pb-based pigments and batteries.[1–3] Due to the ability of the toxic metal to bioaccumulate, poisoning may result from chronic exposure to low levels of Pb.[4,5] After uptake of Pb, it first enters the bloodstream,[2] which upon circulation it distributes the toxic metal to the soft tissues, with liver and kidneys showing the highest level of accumulation. In addition, as Pb is capable of crossing the blood-brain barrier (BBB), it can also be found in the brain.[3,6] Finally, a significant fraction of Pb is stored in calcified tissues, such as bones and teeth, replacing calcium (Ca).[3,7]

Pb acts as a systemic intoxicant, affecting various organs,[7,8] with the nervous system being the most vulnerable target.[1] It was found that children are more susceptible to Pb toxicity related to the central nervous system (CNS), resulting in a range of cognitive deficits.[5,9]

Under physiological conditions, Pb is predominantly found in its cationic state as Pb^{2+}. The toxicity of Pb^{2+} is exerted through an ionic mechanism or *via* induction of oxidative stress,[10,11] with the latter being a result of an imbalance between reactive oxygen species (ROS) and antioxidants. The presence of Pb^{2+} in the cellular environment renders antioxidants like glutathione (GSH) inactive *via* covalent, strong binding.[1,10,11] While interacting with proteins, Pb^{2+} ions have a preference to bind to the thiolate group that is found in the side chain of the amino acid (AA) cysteine (Cys), and to AAs that contain carboxylate groups in their side chains, such as aspartate (Asp) or glutamate (Glu). It can also bind to the backbone oxygen atoms of the amide groups in a multitude of different proteins.[1,7,12] The tight metal binding to the peptidic chain alters the conformation of enzymes, resulting in diminished function.[1,7] Pb^{2+} can also substitute several essential metal ions in metalloproteins, causing their dysfunction as a result of the replacement. A notable example is Ca^{2+} ions, which Pb^{2+} ions outcompete even at picomolar concentrations,[9,12,13] and it is a major reason for Pb-induced neurotoxicity.[9] Pb^{2+} ions also replace Zn^{2+} at the active site of the enzyme δ-aminolevulinic acid dehydratase (ALAD), which takes an essential part in heme biosynthesis. As a result of this metal substitution, Pb poisoning results in anemia.[14] The variety of interactions that Pb can undergo and its wide distribution in the body enable this metal to be a potent toxicant that disturbs many biological processes.[10] It was, therefore, necessary, already at the early stages of medicinal research, to develop treatments against metal poisoning in general and Pb toxicity specifically.

1.1 Chelation Therapy

The current treatment modality for Pb poisoning is chelation therapy; the administration of a drug named a chelating agent to bind the toxic metal, solubilize it and enable the removal of the formed complex from the body.[15–17] An ideal chelating agent should possess several essential characteristics: (a) low toxicity of both the chelating agent and the formed complex, (b) selectivity for the respective metal ion, (c) water solubility of both *apo* and *holo* species, (d) formation of an eliminable complex, and (e) ability to penetrate cells and tissues.[1,6,18] Commonly used chelating agents for the treatment of Pb poisoning are *dimercaprol* (BAL), *3-dimercapto-propanesulphonic acid* (DMPS), *ethylenediaminetetraacetic acid* (EDTA) and *dimercaptosuccinic acid* (DMSA; Figure 1).[6,16–18]

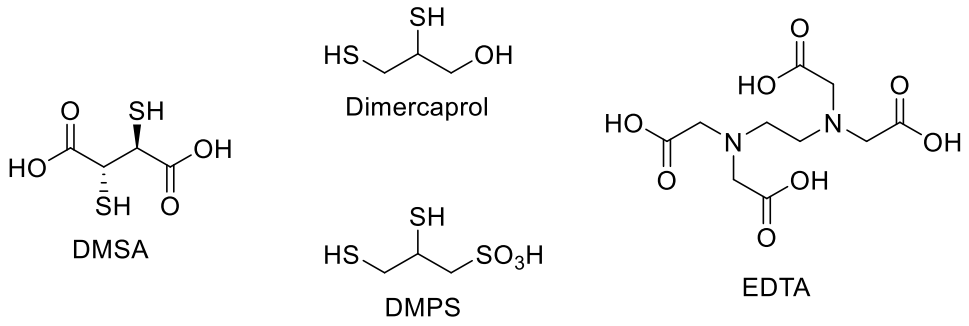

Figure 1 Structures of chelating agents used to treat Pb poisoning

These small-molecule drugs bind the toxic metal *via* their thiolate or carboxylate groups, while accomplishing some of the requirements stated above.[15,17,18] Yet, despite being the primary treatment for Pb poisoning, these drugs suffer significant drawbacks, mainly low metal selectivity that results in essential metals being depleted from the body during treatment. In such cases, this phenomenon can cause toxicity upon drug administration, in addition to the inherent toxicity that some agents show.[16,19] Further, not all chelating agents used for Pb can cross cellular membranes, limiting their use to extracellular targets. An example of that limitation is EDTA that also might redistribute Pb^{2+} ions to the brain.[19]

1.2 Environmental Remediation

Pollution of Pb poses a critical health threat to all ecosystems.[20] Remediation is, therefore, crucial for reducing damage. Techniques for remediation of Pb and other toxic metals from the soil and water are divided into physical, chemical, and biological methodologies.[21]

Bioremediation[22–25] is based on the treatment of contaminated soil or water with organisms, typically bacteria or plants, that are capable of absorbing the contaminant and of subsequently removing it from or reducing its mobility in the environment.[24,26] This modality offers a cost-effective and environmentally friendly way to remediate toxic metals, including Pb.[22] Although

bioremediation is a highly potential approach to treat metallic contaminants, this method suffers from several drawbacks, such as the limited tolerance for toxic metals of the employed organisms, finite root extensions for plants, unsuitable environmental growth conditions and undesired recycling of the metal.[22,27] This yields constant biotechnological attempts to identify new organisms for the purpose, as well as to develop improved strategies and chelating systems that bear higher affinity, resistance, and stability towards Pb.[22,23,25,28]

Chemical remediation covers a wide range of different techniques, such as solidification, stabilization, and soil washing, which spans precipitation and adsorption, in addition to the most common methods that are ion exchange and chelation.[24,26–30] Yet, chemical remediation encounters various challenges such as lack of selectivity, incomplete removal of toxic metals, as well as the generation of toxic waste and the high amount of resources needed,[29,30] all of which encourage the creative design of modern remediation.

1.3 Detecting Pb

Determination of Pb concentration in soil and water is performed, similarly with other metals, by utilizing well established and highly sensitive analytical techniques, such as atomic absorption spectroscopy (AAS), atomic fluorescence spectroscopy (AFS) and inductively coupled plasma-mass spectroscopy (ICP-MS).[20,31–33] Nonetheless, these techniques require expensive equipment and often extensive sample preparation. Further, they only measure the total concentration of the element of interest in a given sample, a value that was found to be less relevant for toxicity in the case of Pb. This is predominantly since the uptake of Pb by organisms is correlated with the free metal ion concentration, rather than the total one.[20,31,32] Thus, the free Pb^{2+} level better indicates on the bioavailability and should therefore be assessed explicitly in novel sensing methods.[34,35]

The development of sensors that allow fast, species-selective and sensitive on-site detection has gained interest over the past years, and novel methods based on an array of different principles were established.[20,31–33,36,37] In addition, several biocompatible sensors for Pb detection in living cells were designed, utilizing primarily fluorescence as their method of detection.[38–41] These show promise for further elucidating the intracellular mechanism by which Pb exerts its toxicity.

By summarizing previous achievements in treating, remediating, and detecting Pb, precise needs for designing next-generation solutions become apparent in all these areas, to overcome their current challenges. To develop such smart applications, a thorough understanding of the

physical and chemical properties of Pb is required. Notably, the underlying principles of the coordination chemistry of Pb should be understood to design novel chemical solutions towards therapeutics, remediation, and diagnostics.

1.4 Physical and Chemical Properties of Pb

Pb has a predominant oxidation state of 2, bearing the electronic configuration [Xe]$4f^{14}5d^{10}6s^2$.[42–44] The ionic radius of Pb^{2+} is 1.19 Å, drastically bigger than most essential metal ions, such as Zn^{2+}, $Cu^{+/2+}$, and $Fe^{2+/3+}$ (in both spin states) and almost similar to the radius of Ca^{2+} (1.12 Å).[44,45] Due to its large ionic radius, Pb^{2+} can be complexed in a wide range of coordination numbers (CN), from 2 to even 12.[44]

The $6s^2$ lone pair of Pb^{2+} ion, which does not participate in binding (as described in the inert pair effect), is stereochemically active at CN at the range of 2 - 5. At these CN, the geometry of the complex is hemidirected, with the ligands occupying one hemisphere of the ion and the lone pair the other (Figure 2a). At higher CN of 9 or above, the ligands are uniformly distributed around the metal ion, leading to a holodirected geometry and rendering the $6s^2$ lone pair stereochemically inactive (Figure 2b).[12,44,46] Complexes that possess intermediate CN of 6 - 8 were found to adopt both geometries.[43]

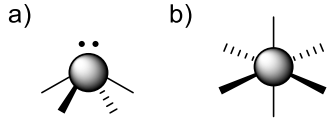

Figure 2 Schematic structures of hemidirected (a) and holodirected (b) Pb complexes

Pb^{2+} is a borderline acid[47] according to the hard-soft acid-base (HSAB) principle and, therefore, exhibits a preference for thiolates as soft ligands, as well as for borderline N and O groups as electron donors in small-molecule ligands and proteins.[8,44,48,49] In several polypeptides, such as GSH, and zinc finger proteins, Pb^{2+} binds thiolate groups of Cys in a tricoordinate fashion.[8] In larger and more complex coordination environments, such as proteins that bind Pb^{2+}, the contributions of other factors than the nature of the binding groups, also play a role. Such factors are the steric and chelate effects, solvent exposure, and flexibility *vs.* rigidity of the metal-binding sites. As a result, a variety of coordination environments has been observed for Pb^{2+}.[12,44] The capability of Pb^{2+} to outcompete Ca^{2+} at binding sites that are natively designed to bind the latter are examples thereof,[12] as these binding sites are oxygen-rich environments, due to the hard nature of Ca^{2+}.

2 Applicable Peptides Against Pb

The prevalence of Pb in the environment and its significant negative impact on ecological systems and human health pose a challenging situation. This complex issue requires novel solutions concerning different aspects, with detection, remediation, and treatment of Pb poisoning being at the forefront, aside from reducing the release of the toxic metal into the environment. Polypeptides provide a versatile toolkit for chemically tackling these problems, with nature providing plenty of scaffolds and, as a great variety of molecules can be created using established routes. Furthermore, polypeptides provide unique coordination spheres for selective and high-affinity binding for a variety of metal ions.[8,48–50] We, therefore, chose to cover selected recent advances in the areas of remediation, detection, and modeling, where peptide or protein design has been applied to these problems (Table 1). Noteworthy, no attempts to design next-generation peptide-based therapeutics against Pb were found to be reported.

Table 1 Peptides described in this review

Peptide	Sequence or Name	Application	Reference
1	$(VK)_3$V-CGPKEC-$(VK)_3$V-NH_2	Remediation by hydrogelation	52
2	TNTLSNN	Remediation by surface display	25
		Electrochemical sensing	58
3	$(EC)_{20}$G	Remediation by surface display	54
4	Cyc-CTNTLSNNC	Electrochemical sensing	59
5	KVSATDADDDVLL	Electrochemical sensing	61
6	Cyc-eEeElLlW	Fluorescent sensing	64
7	Cyc-ElElElEw		
8	Cyc-ElClElCw		
9	TPE-GSSG-TPE	Fluorescent sensing	66
10	E_{23}, E_{215}, E_{500}	Fluorescent sensing	67
11	His_2Cys_2 in PBR	Nanoparticle fluorescence sensing	68
12	PbrR-based system	FRET-based sensing	39
13	3-SCC systems	Model of ALAD enzyme	70
14	3-SCC systems	Model of ALAD enzyme	69
15	Cys_2His_2 model	Model of zinc fingers	73
16	GMTCSGCSRP (linear and cyclic)	Model of Atx1 metallochaperone	75, 77

2.1 Remediating Peptides

Hydrogels are highly absorbent materials composed of networks of hydrophilic polymers. Due to their properties, they serve as an excellent platform for metal remediation applications.[51] Knerr *et al.* reported on the activity of a fully peptidic hydrogel, 20 AAs long, that is composed of three subunits; (a) two identical heptameric fragments with the sequence *$(VK)_3V$*, one at each terminus of the peptide, and (b) the hexamer *CGPKEC* that strongly sequesters various metal ions, including Pb^{2+} in the middle.[52] The termini fragments were *de novo* designed to self-assemble upon formation of β-hairpin, that thanks to the Lys side chains that are hydrophilic and, therefore, H_2O absorbent. The metal-binding fragment, on the other hand, is based on a

natural viral peptide, and that also contains the PG motif that induces a type 1 β-turn. Under reductive condition, the designed peptide (**1**; *(VK)$_3$V-CGPKEC-(VK)$_3$V-NH$_2$*; Figure 3) is capable of binding the metal ion *via* its two Cys residues. Circular dichroism (CD) spectroscopy revealed that while the *apo* form of the peptide exists as a random coil, upon addition of Pb^{2+}, the turn is induced due to the coordinating Cys side chains and the amphiphilic character of the formed complex drives hydrogelation. An equimolar binding ratio was found for CH_3As^{2+}, Zn^{2+}, Cd^{2+}, Hg^{2+} and Pb^{2+}, indicating bidentate binding for all of these metal ions, and the gel was found to be rigid and self-supporting. As a potential use, apart from remediation, this hydrogel may also be applied as a sensor, since the sol-gel transition upon metal binding is easily detected.[52] This example of a smart, proteinogenic peptide that can sequester toxic metal ions and simultaneously change its structure to allow for a functional assembly demonstrates the wide range of capabilities that can be achieved with designed peptides. Yet the high production costs of such peptide needs to be reduced to enable an affordable application.

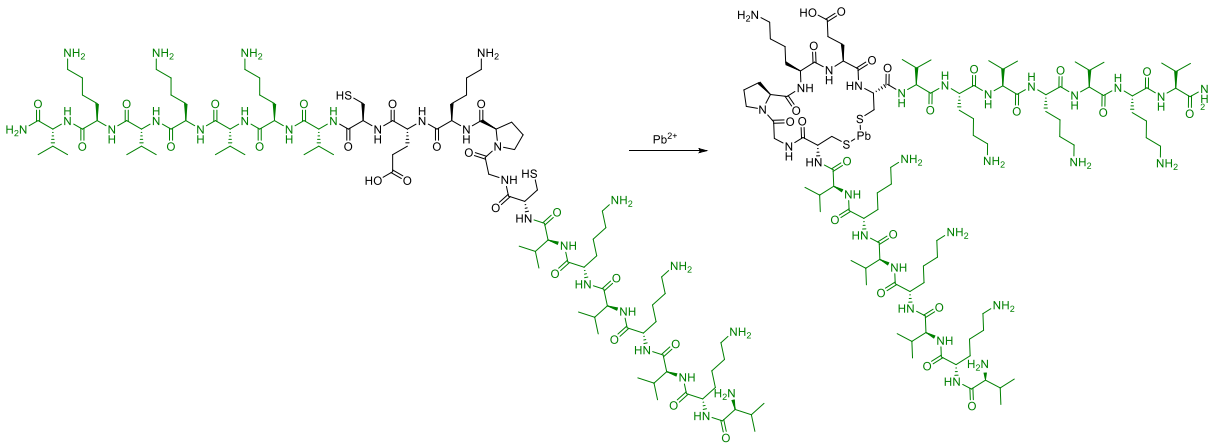

Figure 3 Changes in peptide structure and hydrogelation as a result of Pb^{2+} complexation with **1**[25]

Exploring a different approach, the Pb^{2+} selective heptapeptide *TNTLSNN* **2** was used for surface display in *E. coli,* as an attempt to utilize the peptide-decorated bacteria for bioremediation.[25] For that purpose, the DNA sequence that encodes for this peptide (that was discovered by chromatographic biopanning[53]) was integrated downstream to the 3' end of the *E. coli* outer membrane protein (OmpC) gene by molecular cloning, yielding the recombinant protein OmpC$_t$. Upon expression, the dried cells were tested for metal selectivity and their capacity for Pb^{2+} removal from aqueous solutions. The cells were therefore incubated with single metal solutions containing Pb^{2+}, Co^{2+}, Cu^{2+}, $Ni^{2+,}$ or a solution containing all these metal ions together, and the experiments were compared to wild-type (wt) *E. coli*, expressing no OmpC. Binding kinetics revealed that after 30 min, a binding capacity of 80% was reached, and no significant improvement occurred after 1 h. Analysis of the respective Langmuir-Isotherm

delivered a value of 485.0 μmol g^{-1} dry cells as the maximum absorption capacity for Pb^{2+}, which is reported to be moderate compared to other biological sorbent systems. In single metal solutions, wt *E. coli* had a similar affinity for Pb^{2+} and Cu^{2+} that is 6 times higher compared to the binding affinity of Ni^{2+} and Co^{2+}.

In contrast, the recombinant *E. coli* strain that harbors the gene for $OmpC_t$ revealed an affinity for Pb^{2+} that is at least 4.5 higher than for Cu^{2+}, showing an improved affinity. Further, the recombinant bound lower amounts of Ni^{2+} and Co^{2+} compared to the wt. In the mixed solution, the recombinant was found to bind 6 times more Pb^{2+} than Cu^{2+}, while Ni^{2+} and Co^{2+} binding was negligible. The differences compared to the results of the single metal solutions were attributed to kinetic competition, indicating faster kinetics for Pb^{2+} binding. In comparison with the wt, the **2**-displaying *E. coli* strain adsorbed approximately 3 times more Pb^{2+} ions, showing the effectiveness of the peptide-displaying bacterium as a selective modality for remediation.[25]

In a similar approach, the synthetic phytochelatin (PC) $(EC)_{20}G$ (**3**) was displayed on the surface of the metal-resistant bacterium *C. metallidurans*.[54] Noteworthy, this synthetic molecule differs structurally from its natural counterparts in two crucial perspectives: a) Glu is connected to Cys *via* its α carboxylic group, while in natural PCs they are connected *via* the γ carboxylic group and b) the chain length of the -*EC*- unit extends beyond the ones found in organisms. The DNA sequence coding for this peptide was cloned downstream to the one of an autotransporter protein IgAβ, facilitating translocation through and attachment to the outer membrane. This modified strain was tested for its capability of binding the metal ions Pb^{2+}, Zn^{2+}, Cu^{2+}, Cd^{2+}, Ni^{2+}, $Mn^{2+,}$ and Co^{2+}. **3**-displaying bacteria showed the highest affinity for Pb^{2+} among all tested metal ions. Compared to the unmodified *C. metallidurans*, the amount of bound metal was increased for all metal ions, but was most pronounced for Pb^{2+} and Zn^{2+}, with 547.5 ± 17.1 and 510.7 ± 15.3 1 μmol g^{-1} dry cell, respectively.[54] These values correspond to a 3-fold increase compared to the control and are comparable to other surface-display systems in bacteria[25] and is reported to be among the highest capacities found in modified bacteria.

2.2 Peptidic Sensors for Pb Detection

Three main mechanisms for the detection of Pb are implemented on the reported peptide-based sensors and rely on: (a) immobilized peptide with preformed binding sites (b) assembly of several subunits upon Pb binding, and (c) conformational changes. In all three approaches, the change upon Pb binding is translated to an electrochemical response or fluorescence. Several examples for each mechanism of inspiring designs are herein presented.

Preformed Binding Sites

Short peptides have been used as selective recognition elements for Pb^{2+} in several studies, where they served as sensors in electrochemical methods.[55] In these techniques, peptides are immobilized on the surface of the working electrode for preconcentration of the metal ion and therefore serve as a device for capturing Pb^{2+} ions. The captured ions are subsequently analyzed by voltammetric stripping, a highly sensitive method applicable for metal detection.[56] It involves a deposition step in which the respective metal ion is reduced to its zero-valence state, followed by electrochemical oxidation of the deposited metal. Analyzing the peaks of the oxidative stripping allows for the identification of the metal and its concentration.[57]

The heptapeptide *TNTLSNN* **2**, which was reported to bind Pb^{2+} ions selectively,[53] was used as the recognition element.[58] It was covalently linked *via* its N-terminal amine to a polymer-coated gold (Au)-electrode for functionalization (Figure 4). This high-affinity peptide was found to bind Pb^{2+} with a K_d value of 3.3 x 10^{-11} M at low pH. At pH 3.5 the functionalized electrode was able to selectively detect Pb^{2+} at a concentration of 1 nM against a wide range of other metal ions, including K^+, Ca^{2+}, Cd^{2+}, Co^{2+}, Cu^{2+}, Mg^{2+}, Ni^{2+}, Zn^{2+}, Cr^{3+} and Fe^{3+}, which all were present at a high excess of 50 µM concentration. The device showed a linear response from 1 nM to 10 mM of Pb^{2+}, rendering it highly selective and a strong binder for Pb^{2+}. Interestingly, this peptide does not contain the AAs bearing the functionalities usually coordinating Pb^{2+} in polypeptides, such as thiol, and carboxylic groups, but uncharged hydroxyl and amide functional groups. However, information regarding the coordination site and mode of binding was not reported for **2**.

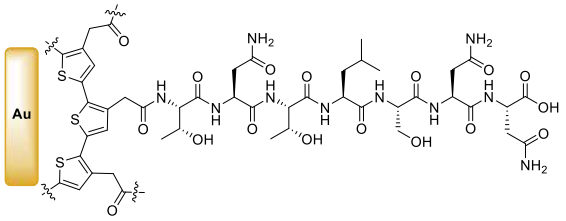

Figure 4 Peptide **2** covalently attached to poly(thiophene acetic acid) that coats a gold electrode for high-affinity electrochemical detection of Pb^{2+} ions[58]

In a different approach to surface functionalization, a self-assembled peptidic layer was fabricated on an Au-electrode. A similar peptide as **2**, but with one Cys residue at each terminus (*CTNTLSNNC,* **4**), was used in this study, while the molecule was cyclized *via* disulfide bridge formation.[59] The formation of a self-assembled peptide layer on the electrode could be confirmed by square-wave voltammetry, and the modified electrode was subsequently examined for selectivity and affinity toward Pb^{2+} at pH 3.5. Experiments revealed that this electrode was highly selective, showing a linear response to Pb^{2+} concentration, ranging from

50 to 700 nM. The limit of detection is slightly higher for this peptide sequence than for its linear counterpart, not bearing Cys residues. It is, however unclear, if this difference is attributed to the peptide sequence alone or due to differences in the apparatus used for detection. A competition experiment in the presence of Pb^{2+}, Ni^{2+}, Cr^{3+}, Cd^{2+}, Ca^{2+}, Mg^{2+}, and K^{+}, each at 500 nM, revealed a remarkable selectivity of this modified electrode for Pb^{2+}. Only little interference by other metal ions occurred, rendering this electrode a promising candidate for Pb^{2+} detection in complex mixtures of metal ions.

In contrast, another study used the short tripeptide GSH, as well as its two fragments *γEC* and *CG*, to modify a graphite-epoxide composite electrode for the simultaneous detection of Pb^{2+}, Cd^{2+} and Zn^{2+} at different pH values (6.8, 7.5 and 8.2).[60] At all pH conditions, the most sensitive peptide for all three metal ions was GSH, followed by *γEC* and only then *CG*, with detection being possible in the ppb range for the former. It could be presumed that both the thiol and the two distant carboxylic groups of GSH together contribute to the high affinity.

Also adopted from a natural protein, the Ca^{2+} binding site found in calcium-dependent adhesion proteins (known as cadherins), the 13 AA-fragment *KVSATDADDDVLL* (**5**) was tested for its capability to selectively detect Pb^{2+} in a complex mixture of metal ions. The peptide was modified with a methylene blue moiety at the C-terminal end and immobilized on an electrode surface *via* an alkanethiol linker at the N-terminus.[61] As the detected current correlates with the distance between the methylene blue moiety and the surface, binding of Pb^{2+} to the peptide reduces its flexibility. It thereby suppresses the measured current as a result of closer proximity between the two components. In contrast to voltammetric stripping, the peptide here acts as a signal switch, directly influencing the measured signal.

Although the exact location and mode of binding is unknown, it has been suggested that Pb^{2+} ion most likely binds to Asp residues, based on the fact that strong interactions between Asp and the metal ion were reported in previous studies.[62,63] The peptide sensor exhibited a dynamic range from 5 – 80 µM, which is relatively high compared to other electrochemical techniques.[58,59] Additionally, this peptide showed remarkable selectivity for Pb^{2+} in a mixture containing Cd^{2+}, Fe^{3+}, Cr^{3+}, Ni^{2+}, Co^{2+}, As^{3+}, Mn^{2+}, Cu^{2+}, Zn^{2+}, Mg^{2+} and Ca^{2+} at equimolar concentrations of 100 µM, rendering it a suitable candidate for real-world application.[61] Despite the native peptide sequence stemming from a Ca^{2+} specific protein, the remarkable selectivity for Pb^{2+} over Ca^{2+} displayed here is consistent with other examples, where Pb^{2+} is known to outcompete Ca^{2+} at concentrations as low as in the picomolar range, particularly in flexible and oxygen-rich binding sites.[9,12,13]

Preformed binding sites were also reported for being applied as recognition elements in techniques using different modes of detection than electrochemical ones. In a study, fluorescence and thermodynamics of three cyclooctapeptides as chemosensors for Pb^{2+} and other metal ions were investigated. The three peptides; *cyc(eEeElLlW)* (**6**; small letters for *D*-AAs), *cyc(ElElElEw)* (**7**) and *cyc(ElClElCw)* (**8**; Figure 5) are strategic variations of each other for probing the effect of coordination site location and the nature of the coordination site on metal binding parameters.[64] **6** contains four Glu residues located on the same side of the macrocycle, while in **7** they are evenly spaced out in the peptide structure. In **8** two opposing Glu residues are substituted with Cys, but is otherwise identical to **7**. The Trp residue serves as a fluorophore, which is quenched upon metal binding and therefore enables detection of Pb^{2+}. Isothermal titration calorimetry (ITC) at 26 °C revealed endothermic $(peptide)_2Pb$ complex formation for **6** and **7**, with complex formation constants of $(2.0 \pm 0.5)\cdot 10^5$ and $(1.5 \pm 0.1)\cdot 10^5$ M^{-1}, respectively. These values were comparable and showed that the position of the Glu residues has no dramatic effect on binding affinity. Complexation was found to be driven by entropic contribution, and π-stacking among Trp residues was noticed as a possible contributor for this binding stoichiometry. Complex formation with **8** revealed the same stoichiometry, but was slightly exothermic. Yet, the heat change was too small for subsequent calculations of thermodynamic parameters. It was therefore hypothesized that the substitution of Glu with Cys might have weakened the interaction between Pb^{2+} and the ligand. Steady-state fluorescence measurements at 350 nm revealed that **6** and **7** show very similar behavior upon titration with Pb^{2+}. Both reached a plateau at around 80% quenching, corresponding to a Pb^{2+} concentration of 200 μM. **8** showed the same trend, but a more moderate curve was recorded. It was noted that the geometry of the formed complex could be responsible for the plateau at about 80% quenching, as Trp may be located in a non-accessible position for the metal ions, prohibiting further quenching. Noteworthy, these peptides were also tested for Cd^{2+} and Hg^{2+}, but an increase in binding affinity was found only for Hg^{2+} upon substituting Glu with Cys, which is in agreement with the HSAB principle.[64]

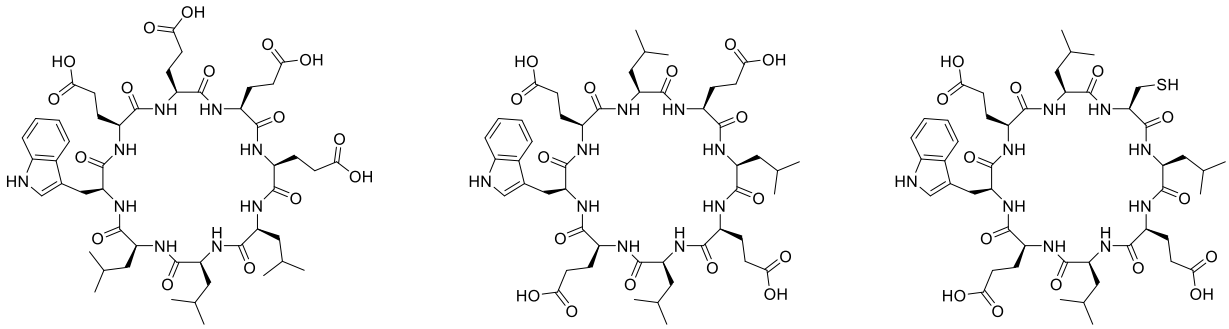

Figure 5 Cyclic octapeptides **6**, **7**, and **8** as fluorescent sensors of Pb^{2+} ions[64]

Another notable design belongs to Wang *et al.* that used the protein Mycobacterium smegmatis porin A (MspA), which is a conical nanopore, for a single ion detection.[65] Position 91 that is located at the pointed end was mutated with either Cys, His or Asp, to have soft, borderline, or hard donors and facilitate metal binding. A monomeric β barrel unit was used for single-channel current recording and, strong binding of Pb^{2+} was recorded with His and Cys that was slightly weaker, but not with Asp.[65] This finding, although congruent with the HSAB principle in simple binding environments, reveals a unique binding pattern with comparison to other Pb-binding peptides and proteins.

Assembly of Subunits

Induction of an assembly of several subunits by a metal ion is an additional application of peptides in sensing techniques. These subunits can be the peptide itself or a peptide-metal complex, that upon assembly, trigger a detectable response. In a detailed study, Gui *et al.* presented a GSH-based fluorescent sensor, which was designed to target the borderline nature of Pb^{2+}.[66] This peptide-fluorophore conjugate TPE-GSSG-TPE (**9**; Figure 6) consists of two GSH subunits bound *via* a disulfide bridge (GSSG), whose two N-termini are modified with the fluorophore tetraphenylethylene (TPE). Upon binding of Pb^{2+}, the complexes aggregate to a supramolecular assembly, which triggers fluorescence emission that allows detection of the metal even at concentrations as low as 1.5 nM.

As GSH contains soft thiol and hard carboxylic groups, that are known to bind a variety of different metal ions, it was hypothesized that oxidation of the two thiol groups would improve the selectivity for Pb^{2+} ion, while conserving the peptides configuration and leaving the remaining four carboxylate groups as coordination sites. The findings agreed with this hypothesis, and a combination of factors, such as the hardness-softness of ligands, coordination geometry, and cavity size – were pointed out as contributors to the observed selectivity. The sensor was tested against its reduced form (TPE-GSH, **9m**; Figure 6) for selectivity towards

Pb^{2+} ions in the presence of different hard, soft, and borderline metal ions. The results showed a high selectivity of the dimer, with only minor interference by Al^{3+}, while **9m** gave signals for all three types of metal ions. Notably, the fluorescence of **9** was higher in the presence of Pb^{2+} than for **9m**, having an estimated K_d value of 2.1 µM.

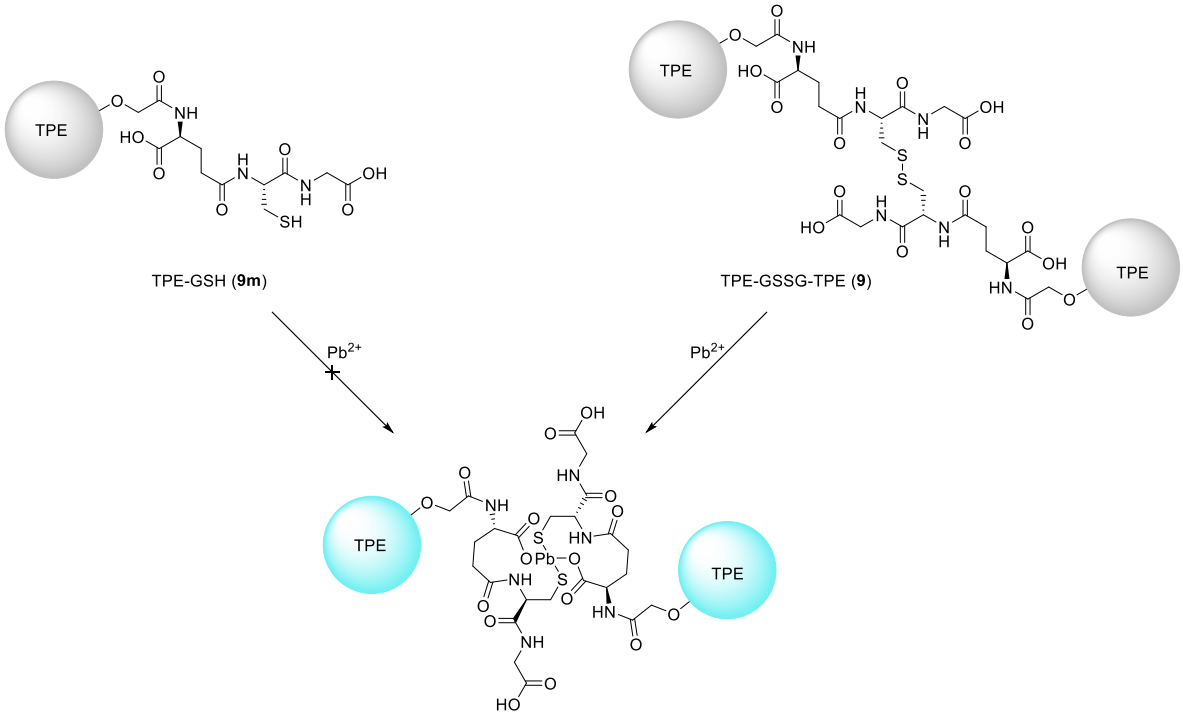

Figure 6 Selective fluorescent detection of Pb^{2+} ions with conjugate **9**[67]

As the thiol groups are oxidized, there are no more soft ligands in the sensor, which would minimize the binding of soft metal ions. For the dimer, interference by Al^{3+} is explained by the fact that Al^{3+} and Pb^{2+} can adopt the same coordination geometry, but Al^{3+} is too small to bind strongly to **9**, giving rise to only weak signals. In contrast, Ca^{2+} did not show any fluorescence, as it prefers CN from 6 to 8, which are not possible with this sensor. Even other borderline acids, such as Fe^{2+} and Cu^{2+} did not bind the dimer, probably due to their small ionic radii, which are not suitable for this ligand, and since their preferred coordination geometries do not match with the device.

FT-IR and MS spectra revealed a 1:1 binding between Pb^{2+} and **9**, while fluorescence measurements revealed fast kinetics, with signal saturation after 60 seconds. Most importantly, due to its biocompatible nature and its low toxicity, the sensor was tested in living cells, where the subcellular distribution of Pb^{2+} could be monitored.[66]

In an example using a simpler design, poly-*L*-Glu (PGA), with 23, 215 and 500 monomeric units (**10**), were investigated with a free fluorophore for the detection of different metal ions.[67] Metal ion binding induces a coil-to-helix formation of the peptide, which leads to its subsequent

aggregation and as a result to the incorporation of the fluorophore. The last step in the process triggers a detectable signal.

The fluorophore that was used is Thiophenephenylanilide-acridinium (TPA) since it can be embedded in hydrophobic pockets of the tertiary structure upon the formation of the assembly. Due to its immobilization in these pockets, the fluorophore emits light at wavelengths that depend on its degrees of motional freedom. This quantity, in turn, is related to the size of the pockets, which varies with the ionic radius and concentration of the intercalating metal ion. These effects allowed for distinguishing different metal ions by the emitted wavelengths. The sensing system is not strictly selective for Pb^{2+}, as Cd^{2+} and Hg^{2+} can also be detected. This sensor is, however, selective for these three metals over several other metal ions, such as K^+, Mg^{2+}, Ca^{2+}, Sr^{2+}, Ba^{2+}, Ag^+, Co^{2+}, Fe^{2+}, and Cu^{2+}.[67] A K_a value of $2.24 \cdot 10^4$ M was detected for the association between Pb^{2+} and PGA with 500 subunits, which binds in a stoichiometry of 1:1. The shorter version of 215 subunits was less capable of forming an enclosed hydrophobic pocket, leading to lower signal intensity, while a 23 AA PGA did not produce any signal, as most likely this sequence was too short of forming hydrophobic pockets upon complexation.[67]

Conformational Change

Conformational changes in polypeptides can also be harnessed to trigger a signal and provide a useful sensing modality. In such an example, ZnS-coated nanoparticles were functionalized with redesigned Phosphate binding protein (PBP) for selective Pb^{2+} sensing in blood plasma.[68] The design of the protein involved placing a His_2Cys_2 binding site in the native PBP sequence (**11**). In addition, adjacent Ser and Thr to this binding site were replaced by Gly, to reduce steric bulk and improve stability. The binding site was designed to accommodate Pb^{2+} in a hemidirected geometry, while disfavoring other geometries, as an attempt to control metal selectivity. Pb^{2+} binding was found to induce a conformational change in this protein, altering the fluorescence of the nanoparticle, which served as the detection entity. The protein was found to be selective for Pb^{2+} over Ca^{2+}, Cd^{2+}, Ni^{2+}, Mg^{2+} and Zn^{2+}, and revealed to be very sensitive with a detection limit of 5 nM. Further, this sensor was successfully implemented in detecting Pb^{2+} in the presence of erythrocytes, emphasizing the potential of such a development.[68]

Another study reported the use of a fluorescence-based sensor (named Met-lead 1.59) that utilizes a part of the natural protein PbrR found in *C. metallidurans* and is known to selectively bind Pb^{2+}.[39] A pair of Förster Resonance Energy Transfer (FRET) proteins was attached to the termini of the chosen metal-binding sequences that were adopted from three isoforms of PbrR metal-binding domains (~70 AAs; **12**), due to their selectivity towards Pb^{2+} and their

conformational change upon Pb^{2+} binding. As a result, the FRET pair becomes closer to each other, causing fluorescence. This sensor was capable of binding two Pb^{2+} ions with dissociation constants K_{d1} and K_{d2} of 69 nM and 22.08 μM, respectively.[39] Selectivity for Pb^{2+} was tested in the presence of various essential metal ions, with only Zn^{2+} showing significant interference that was, however, still distinguishable from Pb^{2+} under physiological conditions. Due to its good selectivity and biocompatibility, this sensor was successfully implemented in live-cell imaging, allowing to monitor Pb^{2+} in the cytosol.

2.3 Peptide Models

Although the routes by which Pb-induced toxicity are partly known, there is still a lot to learn about the exact mechanisms that this metal exerts its poisonous effects.[8] As Pb^{2+} is known to bind a multitude of different proteins, it is essential to study their interactions with this toxic metal, and since working with natural proteins is often challenging, the use of peptides as simplified model systems to study these interactions holds excellent promise. This is thanks to the fact that peptides offer more complexity than small-molecule ligands, but are more accessible to work with than proteins.[8,69] This advantage of peptides as models reveals an additional application, where selected examples are described herein.

To better understand the interaction between Pb^{2+} ions and the Zn binding site of the enzyme ALAD, in which Pb^{2+} substitutes Zn^{2+} and binds to the three Cys residues, several α-helical model peptides that form three-strand coiled-coils (3-SCC) structures (and varied in their sequences and lengths; 23, 29 or 37 AAs; **13**) were studied by ^{207}Pb NMR spectroscopy.[70] Similar to many coiled-coil systems, these peptides are composed of multiple heptad repeats, which form helices. Well-chosen AAs strategically occupy the seven positions in these *abcdefg* repeats: hydrophobic AAs fill positions *a* and *d*, while hydrophilic AAs are placed at *b*, *c,* and *f* sites (Figure 7). AAs with opposing charges occupy positions *e* and *g*, to form stabilizing electronic interactions.[71,72]

For mimicking the tricysteinyl environment that is present in ALAD and other natural proteins that are known to bind Pb^{2+}, Cys residues were incorporated in the peptides at either *a* or *d* positions of the repeats. This enables to control the volume of the metal-binding cavity, where Cys at position *d* results in an enlarged binding site relative to the one placed at position *a*. A PbS_3 coordination environment was identified for both the *a* and *d* substituted peptides. It was, however, found that Pb^{2+} preferentially binds to the larger sites formed by *d* substituted peptides, as these can accommodate the $6s^2$ lone pair of Pb^{2+}. A similar Cys placement is found in ALAD, revealing the importance of the cavity size for Pb^{2+} binding in natural systems.[70]

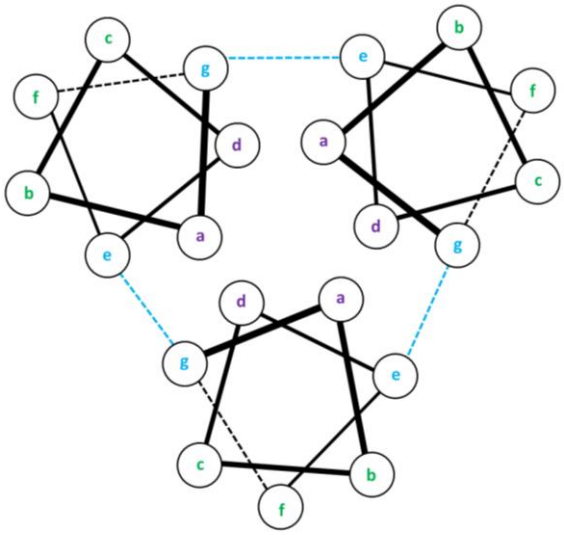

Figure 7 Helical wheel diagram depicting one heptad repeat of a three-stranded α-helical coiled-coil. Hydrophobic positions *a* and *d* are marked in purple, hydrophilic positions *b*, *c,* and *f* are marked in green and charged positions *e* and *g* are marked in cyan.

Pb binding to thiolate-rich sites was further investigated using two similar 30-mer 3-SCC peptides (**14**), each containing one Cys residue in a different location, which are also based on heptad repeat motifs (Figure 7).[69] Utilizing UV-Vis spectroscopy, it was determined that at pH 8, both peptides bind Pb^{2+} ions in a 1:3 metal to peptide ratio, which is consistent with earlier results.[70] Further mechanistic studies of these model systems reveal that at low pH, an intermediate complex is formed, in which only one peptide binds *via* a deprotonated Cys thiolate group and the other two peptides in the complex are neutral. Only at a higher pH, this species simultaneously loses two protons to form thiolate groups and as a result a negatively charged complex. Further investigation of these peptides with Extended X-Ray Absorption Fine Structure (EXAFS) spectra indicated that they are useful models for PbS_3 binding sites in proteins.[69]

NMR spectroscopy was utilized to investigate also the Pb-binding by zinc fingers, using a model peptide that is based on protein Sp1.[73] The 26-meric peptide (**15**) contains a Cys_2His_2 motif, which is a biologically relevant target of Pb^{2+}. It was assumed that this peptide in its *apo* form contains a β-sheet spanning the first 14 AAs, followed by an α-helical structure. 1D NMR spectroscopy suggested that Pb^{2+}, among other metal ions, including Zn^{2+}, was binding to the Cys_2His_2 motif. UV-Vis spectroscopy, however, revealed, that only Pb^{2+} was able to replace Zn^{2+} in this zinc finger domain, while simultaneously adopting the same CN and retain the original tetrahedral geometry.[73] The interaction of Pb^{2+} with this peptide was examined in another study, which underlined these findings.[74]

Another protein that was investigated by its peptidic model for Pb-binding is Atx1, a yeast Cu-metallochaperone.[75] A cyclododecapeptide *cyc*(*GMTCSGCSRP*) (**16**) was designed and

analyzed by NMR spectroscopy and ESI-MS and contains the original binding site *MTCSGCS* of the protein, which is a conserved *MXCXXC* motif, as well as a β-turn inducing *XPGX* motif to rigidify the peptide. Notably, this peptide was found to mimic also the second coordination sphere of Atx1 upon Hg^{2+} binding, as the same hydrogen bond structure as in the native protein was observed.

Coordination occurred *via* the two Cys residues for the ions Hg^{2+}, Cu^{+}, Zn^{2+}, $Cd^{2+,}$ and Pb^{2+}, and a metal to peptide ratio of 1:1 was found for all tested metal ions. The strongest binding was observed for Hg^{2+} and Cu^{+}, while the other metals displayed similar binding affinities that are several orders of magnitude lower than the first two metals. Noteworthy, only at a pH that is higher than 5.5 a complexation with Pb^{2+} and **16** was detected, due to the necessity to deprotonate the thiol groups.[75] This is in contrast to other findings, where Pb^{2+} was able to bind protonated thiols and subsequently inducing deprotonation.[69,76] The higher affinity of the peptide for Cu^{+} and Hg^{2+} is in agreement with the HSAB principle, due to their soft nature.

In a follow-up study, the same peptide, as well as its linear counterpart (**16a**), were further examined to test the effect of cyclization on metal binding.[77] For Pb^{2+} and Cd^{2+} UV-Vis spectra revealed that these metals bind to either two or four thiolate groups, indicating on 1:1 and 1:2 complexation modes. Further, it was noted that both peptides exhibit substantially the same binding behavior, with the **16** reaching higher affinities for the metal ions, probably due to a preorganization of the binding site. The lower affinities for Cd^{2+} and Pb^{2+} than for Hg^{2+} by both peptides are most likely since these metals prefer higher CN than can be provided by these model peptides.

Interestingly, the knowledge acquired so far from peptidic model systems of natural proteins was harnessed for the development of *de novo* designed peptides that Pb^{2+} ions were used for their heteromeric controlled assembly.[78]

3 The Future of Peptides as Chelating Agents

Despite the success in developing peptide-based sensors and remediation devices, and with modeling complexed metalloproteins with their peptide models, to the best of our knowledge, no attempts at using peptides as chelating agents are reported in the literature. There have been, however, examples of polypeptide-based detoxification systems, which consist of surface-displayed proteins[79] and peptide nanomaterials,[80] both successfully lowering Pb burden in mice. As nature harnesses the peptidic scaffold to handle metal toxicity, and since peptide-based drugs have become an impactful strategy to treating various illnesses,[81–83] we anticipate that next-

generation developments of peptide-based chelating agents should be prosperous. This outlook provides considerations from a chemical point of view, as a guideline for the design of peptides as potential chelating agents of Pb.

A successful peptidic chelating agent would have to be designed to target the metal ion of interest with high affinity and selectivity, therefore imposing different chemical and structural requirements to assure these achievements. Several critical parameters concerning the coordination chemistry of Pb^{2+} ion should be taken into account when developing a peptidic ligand, explicitly targeting this metal ion. These parameters can be tailored towards the features of Pb^{2+} and include the nature of the donor atoms or groups, potential CN, coordination geometry, and the size of the binding cavity. As Pb^{2+} is classified as a borderline acid,[47] it is expected to preferentially bind borderline donors from AA sidechains such as His, Asn and Arg. The data presented herein, however, illustrates that Pb^{2+} also tends to bind harder bases, such as carboxylate groups, as well as soft thiolates, both are the most abundant groups coordinating to Pb^{2+} in proteins.[84]

Further, a trend identified throughout this data, shows that the binding sites for Pb^{2+} are mainly constituted by these two functional groups separately, without forming mixed environments. This phenomenon can be identified in the work of Schwemlein *et al*., among others, where the replacement of half the carboxylic acids by thiols resulted in a lowered affinity for Pb^{2+} ions.[64] Likewise, Zhao *et al.* found that blocking thiols in such a mixed site by disulfide bond formation contributed to higher selectivity for Pb^{2+}.[66] Based on this assessment and as opposed to the natural peptide GSH, a successful peptide would likely coordinate Pb^{2+} *via* either carboxylates or thiolates, which are non-coincidentally also present in the small molecule-based chelating agents currently approved for use to treat Pb^{2+} poisoning.[6,16–18]

Importantly, coordination geometry and potential CN that are correlating parameters can be manipulated to enhance the selectivity of a ligand. The hemidirected or holodirected geometries that Pb^{2+} ion adopts for lower and higher CN, respectively,[12,44,46] can be exploited for achieving this purpose. For example, Shete and Benson successfully leveraged this property by choosing structural parameters for a four-coordinated binding site, which favors the hemidirected geometry.[68] With this strategy, selectivity over several other metal ions that are not capable of adopting this geometry was achieved. It is therefore clear that by influencing the complex geometry, binding of undesired metals could be minimized. The same logic applies to the size of the binding site, which has to accommodate this relatively bulky metal ion. Striving for an appropriate size likely reduces the affinity for other metals with different ionic radii than Pb^{2+},

through establishing spatially unfavorable metal-ligand interactions. The importance of this parameter for selectivity has been noted in various works.[66,70]

In addition to its coordination requirements, and regardless of the type of its target, a peptide drug has to withstand degradation by proteases, as a low *in vivo* stability is one of the major drawbacks associated with fully proteinogenic peptides.[85] Various chemical modifications are known for their ability to overcome this issue. These include, among others, the introduction of non-canonical AAs (bearing other functional groups than the ones found in proteinogenic AAs, *D*-AAs, *etc*.),[81,86] backbone modifications (including peptoids) and cyclization.[81] Some of these modifications could simultaneously be utilized to improve other desired features, such as enhancing affinity and selectivity. The most obvious example of this would be the incorporation of nonproteinogenic AAs, as these may not only improve proteolytic stability, but additionally allow introducing new functionalities bearing better-suited donor groups for Pb^{2+} coordination. Together with changing AA configuration, these synthetic modifications may have a critical impact on the binding affinity between metals and ligands, as well as the selectivity of ligands towards Pb^{2+}.[18] Cyclization of the peptide does not only potentially lower proteolytic degradation[81,86] but also rigidifies the structure of the peptide, resulting in a higher level of preorganization and lower degrees of freedom.[77,86] This feature contributed to metal selectivity in various peptides, as the donating groups cannot adapt easily to different metals.[87,88]

Together with an inspiration from natural peptides and proteins, these strategies presented above assemble an initial guideline for the development of selective peptide-based chelating agents of Pb. We hope that the high potential of peptides to act as a remedy towards toxic metals in general and Pb specifically, will be proved beneficial and that new smart designs of such peptidic ligands will be successfully introduced in the future.

4 Acknowledgments

We thank Prof. R. K. O. Siegel and the Department of Chemistry of the University of Zurich for their hospitality and generous support. The Swiss National Science Foundation (SNSF, M. S. S./PZ00P2_179818) and the Forschungskredit of the University of Zurich (L. S./K-73521-11-01) are kindly acknowledged for their financial support.

5 Declaration of interests

The authors declare that they have no known competing financial interests or personal relationships that could have appeared to influence the work reported in this paper.

6 Abbreviations

AA(s)	Amino acid(s)
AAS	Atomic absorption spectroscopy
AFS	Atomic fluorescence spectroscopy
Al	Aluminum
ALAD	δ-aminolevulinic acid dehydratase
As	Arsenic
Au	Gold
Ba	Barium
BAL	British Anti-Lewisite; dimercaptol
BBB	Blood brain barrier
BLL	Blood lead level
Ca	Calcium
Cd	Cadmium
CD	Circular dichroism
CN	Coordination number
CNS	Central nervous system
Co	Cobalt
Cr	Chromium
Cu	Copper
DMPS	Dimercapto-propanesulphonic acid
DMSA	Dimercaptosuccinic acid
EDTA	Ethylenediaminetetraacetic acid
EXAFS	Extended X-Ray Absorption Fine Structure
Fe	Iron
FRET	Förster Resonance Energy Transfer
FT-IR	Fourier-transform infrared
GSH	Glutathione
Hg	Mercury
HSAB	Hard soft acid base
ICP-MS	inductively coupled plasma-mass spectroscopy
ITC	Isothermal titration calorimetry
K	Potassium
Mg	Magnesium
Mn	Manganese
MS	Mass spectrometry
MspA	Mycobacterium smegmatis porin A
Ni	Nickel
OmpC	Outer membrane protein C
Pb	Lead
PBP	Phosphate binding protein
PCs	Phytochelatins
PGA	Poly-*L*-Glu
ROS	Reactive oxygen species
Sr	Strontium
TPA	Thiophenephenylanilide-acridinium
TPE	Tetraphenylethylene
wt	Wild type
Zn	Zinc
3-SCC	Three-strand coiled-coils

6.1 Amino acids

Ala (A)	Alanine	**Leu (L)**	Leucine
Arg (R)	Arginine	**Lys (K)**	Lysine
Asn (N)	Asparagine	**Met (M)**	Methionine
Asp (D)	Aspartic acid	**Pro (P)**	Proline
Cys (C)	Cysteine	**Ser (S)**	Serine
Glu (E)	Glutamic acid	**Thr (T)**	Threonine
Gly (G)	Glycine	**Trp (W)**	Tryptophan
His (H)	Histidine	**Val (V)**	Valine

(1) Flora, S. J. S. *Al Ameen J. Med. Sci.* **2009**, *2* (2), 4–26.

(2) Wani, A. L.; Ara, A.; Usmani, J. A. *Interdiscip. Toxicol.* **2015**, *8* (2), 55–64.

(3) Pfeiffer, R. F.; Zbigniew, W. K.; Manuchair, E. *Parkinson's Disease* 2nd Ed. **2012**. CRC Press.

(4) Mason, L. H.; Harp, J. P.; Han, D. Y. *Biomed Res. Int.* **2014**, 840547.

(5) Lowry, J. A. "Oral chelation therapy for patients with lead poisoning," *Report to World Health Organization*, The Children's Mercy Hospitals and Clinics, Kansas City, Mo, USA, **2010**.

(6) Kim, J. J.; Kim, Y. S.; Kumar, V. *J. Trace Elem. Med. Biol.* **2019**, *54*, 226–231.

(7) Tchounwou, P. B.; Yedjou, C. G.; Patlolla, A. K.; Sutton, D. J. *Mol. Clin. Environ. Toxicol.* **2012**, *101*, 133–164.

(8) Cangelosi, V.; Ruckthong, L.; Pecoraro, V. L. *Metal Ions in Life Sciences Vol. 17,* 1st Ed. **2017**. De Gruyter.

(9) Patrick, L. *Altern. Med. Rev.* **2006**, *11* (1), 2–22.

(10) Jaishankar, M.; Tseten, T.; Anbalagan, N.; Mathew, B. B.; Beeregowda, K. N. *Interdiscip. Toxicol.* **2014**, *7* (2), 60–72.

(11) Flora, G.; Gupta, D.; Tiwari, A. *Interdiscip. Toxicol.* **2012**, *5* (2), 47–58.

(12) Dudev, T.; Grauffel, C.; Lim, C. *Inorg. Chem.* **2018**, *57* (23), 14798–14809.

(13) Godwin, H. A. *Curr. Opin. Chem. Biol.* **2001**, *5* (2), 223–227.

(14) Delahay, R.J.; Spray, C.J. *Proceedings of the Oxford Lead Symposium. Lead Ammunition: understanding and minimising the risks to human and environmental health*. **2015.** Edward Grey Institute.

(15) Aaseth, J.; Ajsuvakova, O. P.; Skalny, A. V.; Skalnaya, M. G.; Tinkov, A. A. *Coord. Chem. Rev.* **2018**, *358*, 1–12.

(16) Flora, S. J. S.; Pachauri, V. *Int. J. Environ. Res. Public Health* **2010**, *7* (7), 2745–2788.

(17) Kaličanin B.; Rašić M.T. *J. Heavy Met. Toxicity Dis.* **2019,** *4* (2:5).

(18) Sears, M. E. *Sci. World J.* **2013**, *2013*, 219840.

(19) Bjørklund, G.; Mutter, J.; Aaseth, J. *Arch. Toxicol.* **2017**, *91* (12), 3787–3797.

(20) Zhou, Y.; Tang, L.; Zeng, G.; Zhang, C.; Zhang, Y.; Xie, X. *Sensors Actuators, B Chem.* **2016**, *223*, 280–294.

(21) Raj, D.; Maiti, S. K. *Environ. Monit. Assess.* **2020**, *192* (2), 108.

(22) Yang, J.; You, S.; Zheng, J. *IOP Conf. Ser. Earth Environ. Sci.* **2019**, *242* (5), 052010.

(23) Naik, M. M.; Dubey, S. K. *Ecotoxicol. Environ. Saf.* **2013**, *98*, 1–7.

(24) Li, C.; Zhou, K.; Qin, W.; Tian, C.; Qi, M.; Yan, X.; Han, W. *Soil Sediment Contam.* **2019**, *28* (4), 380–394.

(25) Nguyen, T. T. L.; Lee, H. R.; Hong, S. H.; Jang, J. R.; Choe, W. S.; Yoo, I. K. *Appl. Biochem. Biotechnol.* **2013**, *169* (4), 1188–1196.

(26) Fu, F.; Wang, Q. *J. Environ. Manage.* **2011**, *92* (3), 407–418.

(27) Akpor, O. B.; Muchie, M. *Int. J. Phys. Sci.* **2010**, *5* (12), 1807–1817.

(28) Mejáre, M.; Bülow, L. *Trends Biotechnol.* **2001**, *19* (2), 67–73.

(29) Malachowski, L.; Stair, J. L.; Holcombe, J. A. *Pure Appl. Chem.* **2004**, *76* (4), 777–787.

(30) A. Waris, A.; Athar, T.; Nisar, M. *Emergent Life Sci. Res.* **2018**, *4* (2), 45–50.

(31) Kim, H. N.; Ren, W. X.; Kim, J. S.; Yoon, J. *Chem. Soc. Rev.* **2012**, *41* (8), 3210–3244.

(32) Priyadarshini, E.; Pradhan, N. *Sensors Actuators, B Chem.* **2017**, *238*, 888–902.

(33) Gumpu, M. B.; Sethuraman, S.; Krishnan, U. M.; Rayappan, J. B. B. *Sensors Actuators, B Chem.* **2015**, *213*, 515–533.

(34) Kalis, E. J. J.; Weng, L.; Dousma, F.; Temminghoff, E. J. M.; Van Riemsdijk, W. H. *Environ. Sci. Technol.* **2006**, *40* (3), 955–961.

(35) Slaveykova, V. I.; Wilkinson, K. J. *Environ. Sci. Technol.* **2002**, *36* (5), 969–975.

(36) De Acha, N.; Elosúa, C.; Corres, J. M.; Arregui, F. J. *Sensors* **2019**, *19* (3), 599.

(37) Li, M.; Gou, H.; Al-Ogaidi, I.; Wu, N. *ACS Sustain. Chem. Eng.* **2013**, *1* (7), 713–723.

(38) Son, H.; Lee, H. Y.; Lim, J. M.; Kang, D.; Han, W. S.; Lee, S. S.; Jung, J. H. *Chem. Eur. J.* **2010**, *16* (38), 11549–11553.

(39) Chiu, T. Y.; Yang, D. M. *Toxicol. Sci.* **2012**, *126* (2), 436–445.

(40) Anand, T.; Sivaraman, G.; Mahesh, A.; Chellappa, D. *Anal. Chim. Acta.* **2015**, *853*, 596–601.

(41) Miller, E. W.; He, Q.; Chang, C. J. *Nat. Protoc.* **2008**, *3* (5), 777–783. https://doi.org/10.1038/nprot.2008.43.

(42) Tangahu, B. V.; Sheikh Abdullah, S. R.; Basri, H.; Idris, M.; Anuar, N.; Mukhlisin, M. *Int. J. Chem. Eng.* **2011**, *2011,* 939161.

(43) Shimoni-Livny, L.; Glusker, J. P.; Bock, C. W. *Inorg. Chem.* **1998**, *37* (8), 1853–1867.

(44) Claudio, E. S.; Godwin, H. A.; Magyar, J. S. *Progress in Inorganic Chemistry, Vol. 51, Chapter 1* 1st Ed. **2002**. Wiley.

(45) Davidovich, R. L.; Stavila, V.; Marinin, D. V.; Voit, E. I.; Whitmire, K. H. *Coord. Chem. Rev.* **2009**, *253* (9–10), 1316–1352.

(46) Zampella, G.; Neupane, K. P.; De Gioia, L.; Pecoraro, V. L. *Chem. Eur. J.* **2012**, *18* (7), 2040–2050.

(47) Kirberger, M.; Yang, J. J. *J. Inorg. Biochem.* **2008**, *102* (10), 1901–1909.

(48) Szunyog, G.; Várnagy, K. *Inorg. Chim. Acta* **2018**, *472*, 157–164.

(49) Lihi, N.; Lukács, M.; Raics, M.; Szunyog, G.; Várnagy, K.; Kállay, C. *Inorg. Chim. Acta* **2018**, *472*, 165–173.

(50) Andreini, C.; Cavallaro, G.; Lorenzini, S.; Rosato, A. *Nucleic Acids Res.* **2013**, *41*, 312–319.

(51) Muya, F. N.; Sunday, C. E.; Baker, P.; Iwuoha, E. *Water Sci. Technol.* **2016**, *73* (5), 983–992.

(52) Knerr, P. J.; Branco, M. C.; Nagarkar, R.; Pochan, D. J.; Schneider, J. P. *J. Mater.*

Chem. **2012**, *22* (4), 1352–1357.

(53) Nian, R.; Kim, D. S.; Nguyen, T.; Tan, L.; Kim, C. W.; Yoo, I. K.; Choe, W. S. *J. Chromatogr. A* **2010**, *1217* (38), 5940–5949.

(54) Biondo, R.; Da Silva, F. A.; Vicente, E. J.; Souza Sarkis, J. E.; Schenberg, A. C. G. *Environ. Sci. Technol.* **2012**, *46* (15), 8325–8332.

(55) March, G.; Nguyen, T. D.; Piro, B. *Biosensors* **2015**, *5* (2), 241–275.

(56) Pan, D.; Wang, Y.; Chen, Z.; Lou, T.; Qin, W. *Anal. Chem.* **2009**, *81* (12), 5088–5094.

(57) Borrill, A. J.; Reily, N. E.; Macpherson, J. V. *Analyst* **2019**, *144* (23), 6834–6849.

(58) Su, W.; Cho, M. S.; Nam, J. Do; Choe, W. S.; Lee, Y. *Biosens. Bioelectron.* **2013**, *48*, 263–269.

(59) Lin, M.; Cho, M.; Choe, W. S.; Lee, Y. *Electroanalysis* **2016**, *28* (5), 998–1002. https://doi.org/10.1002/elan.201500574.

(60) Serrano, N.; Prieto-Simón, B.; Cetó, X.; Del Valle, M. *Talanta* **2014**, *125*, 159–166.

(61) Lotfi Zadeh Zhad, H. R.; Lai, R. Y. *Anal. Chem.* **2018**, *90* (11), 6519–6525.

(62) Yusof, N. A.; Daud, N.; Saat, S. Z. M.; Tee, T. W.; Abdullah, A. H. *Int. J. Electrochem. Sci.* **2012**, *7* (11), 10358–10364.

(63) Gasque, L.; Bernès, S.; Ferrari, R.; De Barbarín, C. R.; De Jesús Gutiérrez, M.; Mendoza-Díaz, G. *Polyhedron* **2000**, *19* (6), 649–653.

(64) Ngu-Schwemlein, M.; Gilbert, W.; Askew, K.; Schwemlein, S. *Bioorganic Med. Chem.* **2008**, *16* (10), 5778–5787.

(65) Wang, S.; Cao, J.; Jia, W.; Guo, W.; Yan, S.; Wang, Y.; Zhang, P.; Chen, H. Y.; Huang, S. *Chem. Sci.* **2020**, *11* (3), 879–887.

(66) Gui, S.; Huang, Y.; Zhu, Y.; Jin, Y.; Zhao, R. *ACS Appl. Mater. Interfaces* **2019**, *11* (6), 5804–5811.

(67) Hu, J.; Elioff, M. S. *Talanta* **2018**, *188*, 552–561.

(68) Shete, V. S.; Benson, D. E. *Biochemistry* **2009**, *48* (2), 462–470.

(69) Matzapetakis, M.; Ghosh, D.; Weng, T. C.; Penner-Hahn, J. E.; Pecoraro, V. L. *J. Biol. Inorg. Chem.* **2006**, *11* (7), 876–890.

(70) Neupane, K. P.; Pecoraro, V. L. *Angew. Chem. Int. Ed.* **2010**, *49* (44), 8177–8180.

(71) Hong, J.; Kharenko, O. A.; Ogawa, M. Y. *Inorg. Chem.* **2006**, *45* (25), 9974–9984.

(72) Mocny, C. S.; Pecoraro, V. L. *Acc. Chem. Res.* **2015**, *48* (8), 2388–2396.

(73) Razmiafshari, M.; Zawia, N. H. *Toxicol. Appl. Pharmacol.* **2000**, *166* (1), 1–12.

(74) Razmiafshari, M.; Kao, J.; D'Avignon, A.; Zawia, N. H. *Toxicol. Appl. Pharmacol.* **2001**, *172* (1), 1–10.

(75) Sénèque, O.; Crouzy, S.; Boturyn, D.; Dumy, P.; Ferrand, M.; Delangle, P. Novel *Chem. Commun.* **2004**, *4* (7), 770–771.

(76) Chakraborty, S.; Yudenfreundkravitz, J.; Thulstrup, P. W.; Hemmingsen, L.; Degrado, W. F.; Pecoraro, V. L. *Angew. Chem. Int. Ed.* **2011**, *50* (9), 2049–2053.

(77) Rousselot-Pailley, P.; Sénèque, O.; Lebrun, C.; Crouzy, S.; Boturyn, D.; Dumy, P.; Ferrand, M.; Delangle, P. *Inorg. Chem.* **2006**, *45* (14), 5510–5520.

(78) Tolbert, A. E.; Ervin, C. S.; Ruckthong, L.; Paul, T. J.; Jayasinghe-Arachchige, V. M.; Neupane, K. P.; Stuckey, J. A.; Prabhakar, R.; Pecoraro, V. L. *Nat. Chem.* **2020**, *12*, 405-411.

(79) Hui, C.; Guo, Y.; Zhang, W.; Gao, C.; Yang, X.; Chen, Y.; Li, L.; Huang, X. *Sci. Rep.* **2018**, *8* (1), 1–12. https://doi.org/10.1038/s41598-018-24134-3.

(80) Li, L.; Wu, J.; Zhao, M.; Wang, Y.; Zhang, H.; Zhang, X.; Gui, L.; Liu, J.; Mair, N.; Peng, S. *Chem. Res. Toxicol.* **2012**, *25* (9), 1948–1954.

(81) Lee, A. C. L.; Harris, J. L.; Khanna, K. K.; Hong, J. H. *Int. J. Mol. Sci.* **2019**, *20* (10), 1–21.

(82) Latham, P. W. *Nat. Biotechnol.* **1999**, *17* (8), 755–757.

(83) Henninot, A.; Collins, J. C.; Nuss, J. M. *J. Med. Chem.* **2018**, *61* (4), 1382–1414.

(84) Yu, F.; Cangelosi, V. M.; Zastrow, M. L.; Tegoni, M.; Plegaria, J. S.; Tebo, A. G.; Mocny, C. S.; Ruckthong, L.; Qayyum, H.; Pecoraro, V. L. *Chem. Rev.* **2014**, *114* (7), 3495–3578.

(85) Jensen, K. J. *Peptide and Protein Design for Biopharmaceutical Applications, Chapter 11*st Ed. **2009**. Wiley.

(86) Rohrbacher, F.; Deniau, G.; Luther, A.; Bode, J. W. *Chem. Sci.* **2015**, *6* (8), 4889–4896.

(87) Dudev, T.; Lim, C. *Chem. Rev.* **2014**, *114* (1), 538–556.

(88) Ruckthong, L.; Zastrow, M. L.; Stuckey, J. A.; Pecoraro, V. L. *J. Am. Chem. Soc.* **2016**, *138* (36), 11979–11988.

Graphical Abstract

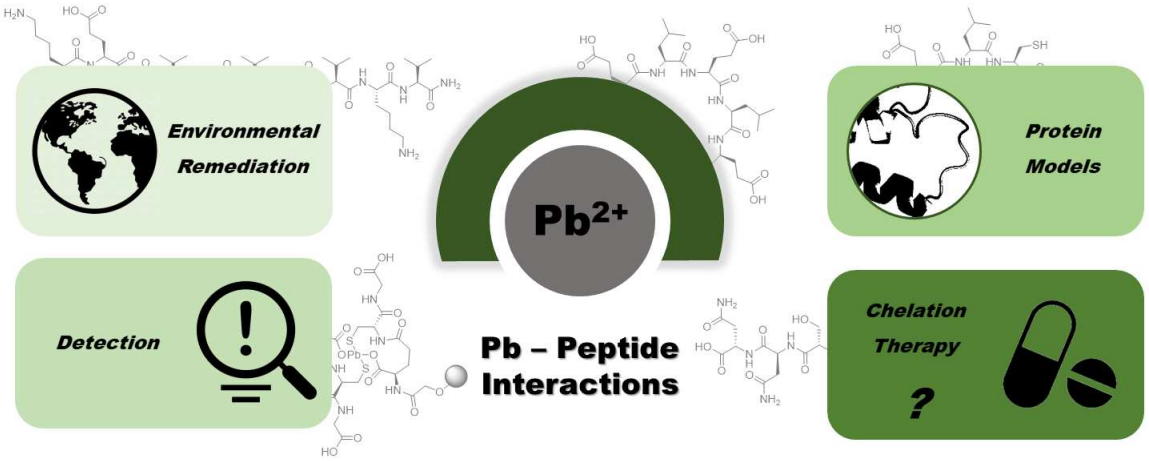

Peptides were developed for handling lead (Pb) pollution and poisoning, in various applications, including in environmental remediation, detection, and modeling. This overview summarizes selected examples of these achievements and also presents a useful guideline, based on these systems, for the design of next-generation, applicable peptides against this toxic metal.